the baculovirus expression vector pVL1393 (Invitrogen) with a His tag at the COOH-terminal end. Proteins were purified by Ni-affinity chromatography (Qiagen). STATs 1, 5, and 6 were expressed and purified by identical methods. For DNA binding studies, insect cells were infected with recombinant viruses encoding JAK1 and one of the STATs.
10. T. K. Blackwell and H. Weintraub, *Science* **250**, 1104 (1990).
11. The optimal STAT4 binding site was selected from a pool of oligonucleotides with random bases at 14 adjacent positions. The bound sequences were separated from the unbound by gel mobility–shift. After three rounds of selection the bound fragments were cloned, and 18 independent isolates were sequenced. All 18 fragments displayed the same 9-nucleotide consensus binding sequence, TTCCGGGAA.
12. J. N. Ihle, *Cell* **84**, 331 (1996); U. Schindler, unpublished results.
13. M. H. Kaplan, Y.-L. Sun, T. Hoey, M. J. Grusby, *Nature* **382**, 162 (1996).
14. P. Gray and D. V. Goeddel, *Nature* **298**, 859 (1982).
15. H. A. Young *et al.*, *J. Immunol.* **143**, 2389 (1989).
16. K. J. Hardy, B. M. Peterlin, R. E. Atchinson, J. D. Stobo, *Proc. Natl. Acad. Sci. U.S.A.* **82**, 8173 (1985); T. Hoey and Y.-L. Sun, unpublished results.
17. The binding reactions were carried out in 50 mM KCl, 12.5 mM Hepes (pH 7.9), 0.1 mM EDTA, 5% glycerol, 0.01% NP-40, 1 mM $NaVO_4$, 1 mM NaF, 1 mM β-glycerophosphate, and 1 μg of poly(dI-dC). The amount of STAT proteins in the binding reactions was between 50 and 500 ng. Only a small fraction of the purified STAT proteins was tyrosine phosphorylated and active for DNA binding. A Hind III to Sac I fragment that was labeled at the Hind III site was used for the footprints.
18. Gel mobility–shift reactions were done with the same buffer as used for the footprint reactions with the addition of 2 mM $MgCl_2$. The sequences of the oligonucleotides were as follows: the high-affinity single site, TTATGTTTCCGGGAAATGAG; site 2 + 3, CGCGAAAATTTTAAGTGAATTTTTTGAGTTTCTTTTAAAATTTT; site 2* + 3, CGCGAAAATTgAGTGgTTTTTTTGAGTTTCTTTTAAAATTTT; and site 2 + 3*, CGCGAAAATTTTAAGTGAATTTTTTTGAGTccCTTTTttAATTTT. The positions of the consensus binding sites are underlined, and the positions of the altered bases are in lowercase letters. The antibodies used in Fig. 4A were obtained from Santa Cruz Biotechnology.
19. S. H. Chan, M. Kobayashi, D. Santoli, B. Perussia, G. Trinchieri, *J. Immunol.* **148**, 92 (1992); K. J. Hardy and T. Sawada, *J. Exp. Med.* **170**, 1021 (1989); C.-S. Hsieh *et al.*, *Science* **260**, 547 (1993).
20. COS-7 cells were transfected by the calcium phosphate precipitation method. Full-length STAT4 and the NH_2-terminal deletion mutant were cloned into the cytomegalovirus vector pRK-5. JAK1 was expressed from the plasmid pSRα. Luciferase reporter plasmids contained either two copies of the site 2 + 3 oligonucleotide or two copies of a high-affinity STAT site upstream of the herpes simplex virus thymidine kinase basal promoter (−50 to +10) in pGL2-basic. The high-affinity STAT site was derived from the IRF-1 promoter, GCCGTCATTTCGGGGAAATCA [S. H. Sims, Y. Cha, M. F. Romine, P. E. Gao, K. Gottleib, A. B. Deisseroth, *Mol. Cell. Biol.* **13**, 690 (1993)]. Each transfection contained 1.5 μg of the STAT4 and luciferase plasmids and 1 μg of Rous sarcoma virus β-galactosidase. The transfections with the IFN-γ sites also included 0.5 μg of the JAK1 expression vector. Transfection efficiencies were standardized by measurement of β-galactosidase activity.
21. X. Xu, Y.-L. Sun, T. Hoey, unpublished results.
22. The sequence within the region protected by STAT1 and STAT4 is AGTCCTTGAATGGTGTGAAGTAAAAGTGCCTT*CAAAG*AATCCCC. The positions with the best match to the consensus binding site are underlined. Two nucleotides in the downstream site indicated by the asterisks were changed in the mutant fragment. The T was deleted and the G was changed to C.
23. Multiple STAT binding sites were detected by DNase I footprint analysis within a Kpn I to Acc I fragment from the downstream intron. Among these sites was a pair of sites that was specifically recognized by STAT1. The sequence with the protected region was ACCTTCTTTGCTCCAAAACTCTACAATGCAAAG*AATAGA, which corresponds to the sequence for the gel shift in Fig. 3C. A single point mutation was made by changing the G (indicated by the asterisk) to C.
24. A portion of the STAT4 cDNA encoding amino acids 1 to 124 with a His tag at the COOH-terminal end was subcloned into the T7 promoter expression vector pET-3A. Protein was expressed in the strain BL21(DE3) and purified by Ni-affinity chromatography.
25. We acknowledge K. Williamson for DNA sequencing and M. Rothe for help with cloning human STAT4. We thank U. Schindler, M. Rothe, T. Mikita, and S. McKnight for comments on the manuscript and helpful discussions, and Genetics Institute for IL-12. B. Schreiber and D. Goeddel provided valuable advice and reagents.

28 February 1996; accepted 19 June 1996

Diffusional Mobility of Golgi Proteins in Membranes of Living Cells

Nelson B. Cole, Carolyn L. Smith, Noah Sciaky,* Mark Terasaki, Michael Edidin, Jennifer Lippincott-Schwartz†

The mechanism by which Golgi membrane proteins are retained within the Golgi complex in the midst of a continuous flow of protein and lipid is not yet understood. The diffusional mobilities of mammalian Golgi membrane proteins fused with green fluorescent protein from *Aequorea victoria* were measured in living HeLa cells with the fluorescence photobleaching recovery technique. The diffusion coefficients ranged from 3×10^{-9} square centimeters per second to 5×10^{-9} square centimeters per second, with greater than 90 percent of the chimeric proteins mobile. Extensive lateral diffusion of the chimeric proteins occurred between Golgi stacks. Thus, the chimeras diffuse rapidly and freely in Golgi membranes, which suggests that Golgi targeting and retention of these molecules does not depend on protein immobilization.

The Golgi complex contains a large number of resident components that play important roles in the processing and sorting of secretory and membrane proteins, but how these components are maintained in the Golgi despite a continuous flow of protein and lipid through the secretory pathway is currently a topic of debate (*1*). Several mechanisms of Golgi protein retention have been suggested: oligomerization into structures too large to enter transport vesicles (*2*), lateral segregation into lipid microdomains (*3*), and recognition of retention or retrieval signals (*4*). In these models specific protein-protein or protein-lipid interactions underlie Golgi protein retention. Whether such interactions affect the dynamic properties of Golgi membrane proteins in vivo, including the diffusional mobility of Golgi proteins and trafficking of these proteins between Golgi stacks, has not been addressed.

N. B. Cole, N. Sciaky, J. Lippincott-Schwartz, Cell Biology and Metabolism Branch, National Institute of Child Health and Human Development, Building 18T, National Institutes of Health, Bethesda, MD 20892, USA.
C. L. Smith, National Institute of Neurological Disorders and Stroke, Building 36, National Institutes of Health, Bethesda, MD 20892, USA.
M. Terasaki, Department of Physiology, University of Connecticut Health Center, Farmington, CT 06032, USA.
M. Edidin, Department of Biology, The Johns Hopkins University, Baltimore, MD 21218, USA.

*Present address: National Jewish Center for Immunology and Respiratory Medicine, 1400 Jackson Street, Denver, CO 80206, USA.
†To whom correspondence should be addressed. E-mail: jlippin@helix.nih.gov

To probe for interactions that might underlie the retention of Golgi membrane proteins, we examined the diffusional mobility of Golgi membrane components using fluorescence photobleaching recovery (FPR). This technique is a powerful tool for investigating the environment of membrane proteins and has revealed several types of interactions that constrain the lateral diffusion of proteins in the plasma membrane (*5*). The dynamic properties of intracellular membrane proteins have not been thoroughly explored by FPR because of a lack of appropriate fluorescent labels. Here, we used the *Aequorea victoria* green fluorescent protein (GFP) (*6*) as a tag to investigate the diffusional mobility of four Golgi membrane proteins (*7*), mannosidase II (Man II), β-1,4-galactosyltransferase (GalTase), and wild-type and mutant forms of KDEL receptor (KDELR), within the Golgi and the endoplasmic reticulum (ER). We also used fluorescence loss in photobleaching to examine the extent of lateral membrane continuity between Golgi stacks, and within the ER.

Man II and GalTase are "resident" enzymes of the Golgi complex, which function in carbohydrate processing. In contrast, KDELR is an itinerant Golgi component, which recycles to the ER when it binds KDEL ligand (*8*). Substitution of asparagine for aspartic acid at position 193 in KDELR, denoted $KDELR_m$, prevents it from redistributing into the ER in the presence of high concentrations of ligand (*9*). GFP was fused

to full-length Man II at its lumenally oriented COOH-terminus (Man II–GFP), to GalTase truncated at position 60 in its lumenal domain (GalTase-GFP), and to the cytoplasmically oriented COOH-terminus of wild-type (KDELR-GFP) and mutated KDELR ($KDELR_m$-GFP) (*10*).

When each of the GFP-tagged proteins was expressed in HeLa cells, fluorescence was localized almost exclusively to juxtanuclear Golgi structures (Fig. 1, A to D). Observations in cells treated with brefeldin A (BFA), which causes Golgi membranes but not other membranes to redistribute into the ER (*11*), further supported a Golgi localization of the GFP chimeras (Fig. 1, E and F). Overexpression of lysozyme-KDEL (ligand for KDELR) caused KDELR-GFP, but not $KDELR_m$-GFP, to redistribute into the ER (Fig. 1, G and H), as observed in previous studies characterizing wild-type and defective KDEL receptors (*9*). Thus, the GFP tag did not interfere with Golgi targeting of KDELR, Man II, and GalTase or with ligand-induced recycling of KDELR.

The diffusional mobilities of the GFP chimeras within Golgi membranes were examined in living cells at 37°C by bleaching out fluorescence in a Golgi region with a high-energy laser scan of a confocal microscope and then using lower intensity illumination to image the recovery of fluorescence by means of diffusion of unbleached GFP chimeras into this region. Fluorescence recovery into the photobleached region was rapid for all of the GFP chimeras (Fig. 2). The mobile fraction of

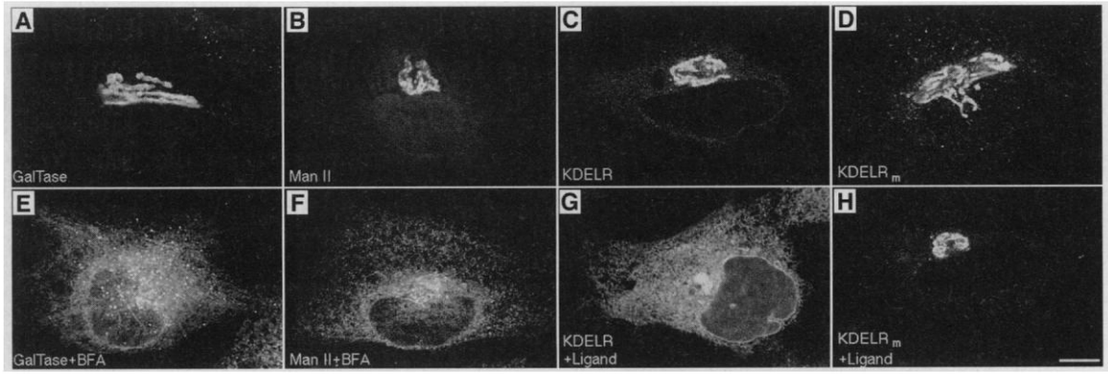

Fig. 1. Expression of Golgi-targeted GFP chimeras revealed by fluorescence microscopy of living HeLa cells transfected with GalTase-GFP, Man II–GFP, KDELR-GFP, or $KDELR_m$-GFP (*26*). (**A** to **D**) Chimera distributions in untreated cells. Distributions of GalTase-GFP (**E**) and Man II–GFP (**F**) after a 30-min treatment with BFA (2 μg/ml), and KDELR (**G**) or $KDELR_m$ (**H**) after overexpression of lysozyme-KDEL (ligand). Each of the chimeras colocalized extensively with native protein labeled with antibodies in untreated, fixed cells. Scale bar = 10 μm.

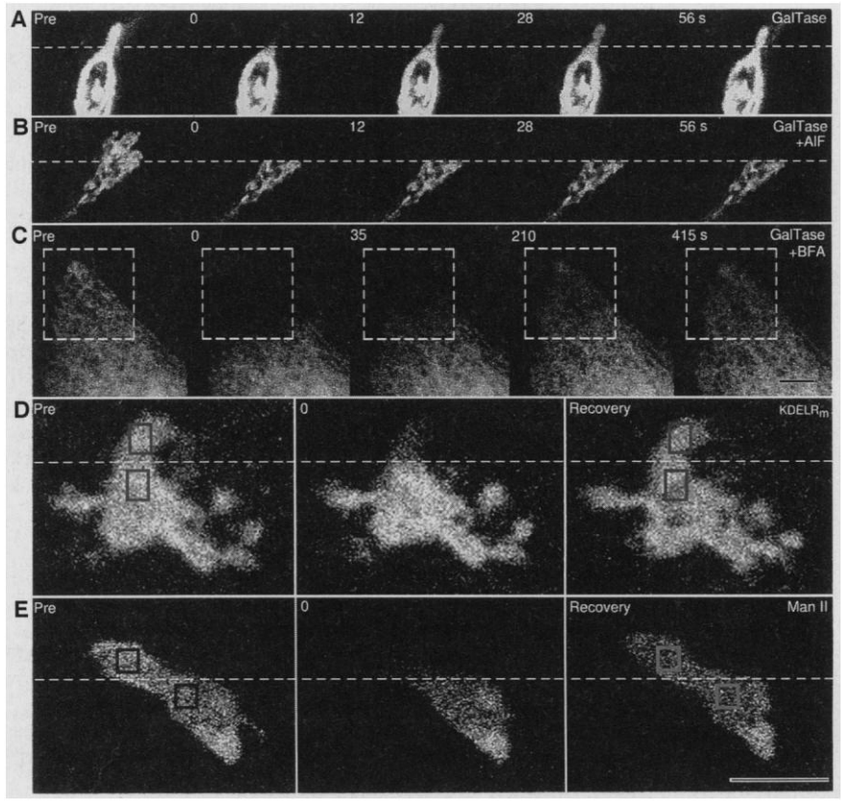

Fig. 2. Fluorescence photobleaching recovery of GFP chimeras in Golgi and ER membranes. Sequence of images of GalTase-GFP in Golgi of a control cell (**A**) and an AlF-treated cell (**B**) before and after photobleaching. The region of Golgi above the dotted line was photobleached immediately after the first image (Pre). In (A) the photobleached area rapidly recovered fluorescence, whereas in (B) there was essentially no recovery. (**C**) Sequence of images of GalTase-GFP in the ER of a BFA-treated cell before (Pre) and after photobleaching of the boxed region. Fluorescence returned to the photobleached region of the ER in BFA-treated cells whether or not AlF was present. The region of Golgi above the dotted line in (A) and (B) or of ER within the boxed area in (C) was photobleached by scanning it three times with the highest laser energy (100% power, 100% transmission). Recovery of fluorescence into the photobleached region was then observed by imaging the entire Golgi element at low energy (10% power, 3% transmission) at the times indicated after the bleach. Before photobleaching, the cells in (B) were treated with AlF (30 mM NaF and 50 μM $AlCl_3$) for 30 min, and in (C) they were treated with BFA (2 μg/ml) for 1 hour. (**D** and **E**) Method used to calculate mobile fraction of GFP chimeras. Fluorescence intensities in the boxed regions of interest (ROIs) were measured before bleaching (Pre) and after recovery (Recovery). The ratio of bleached to unbleached ROIs at these two time points were used to calculate the mobile fraction (mobile fraction = ratio after recovery/ratio before bleaching). For $KDELR_m$-GFP, the mobile fraction was 98%, whereas for Man II–GFP it was 90%. The absolute fluorescence associated with Golgi elements was lower after photobleaching than before photobleaching because photobleaching removed a significant proportion of total fluorescence from the Golgi. The method described above for calculating mobile fraction is insensitive to this loss. Scale bar in (C) is equivalent to 10 μm in (C) and 5 μm in (A) and (B). Scale bar in (E) is 5 μm for (D) and (E). A Quicktime movie sequence from the FPR experiment is available at http://www.uchc.edu/htterasaki/flip.html.

GFP chimeras was determined in a series of images by calculating the ratio of fluorescence intensities for two regions of interest, one within the bleaching zone and the other outside of it, before photobleaching and after recovery (see boxed areas in Fig. 2, D and E, for GFP-KDELR$_m$ and GFP-Man II, respectively). The ratio after recovery ranged between 85 to 98% of the ratio before photobleaching in multiple experiments performed with all of the chimeras. Thus, nearly all of the GFP chimeras were mobile in Golgi membranes. Recovery was due to diffusion within a continuous membrane compartment rather than transfer of fluorescence by fusion of unbleached vesicles with the bleached region, because fluorescence recovered at the same rate in cells at reduced temperatures (22°C) or upon energy depletion with a mixture of 2-deoxyglucose and sodium azide, conditions where vesicle transport has been found to be significantly slowed or blocked (*12*).

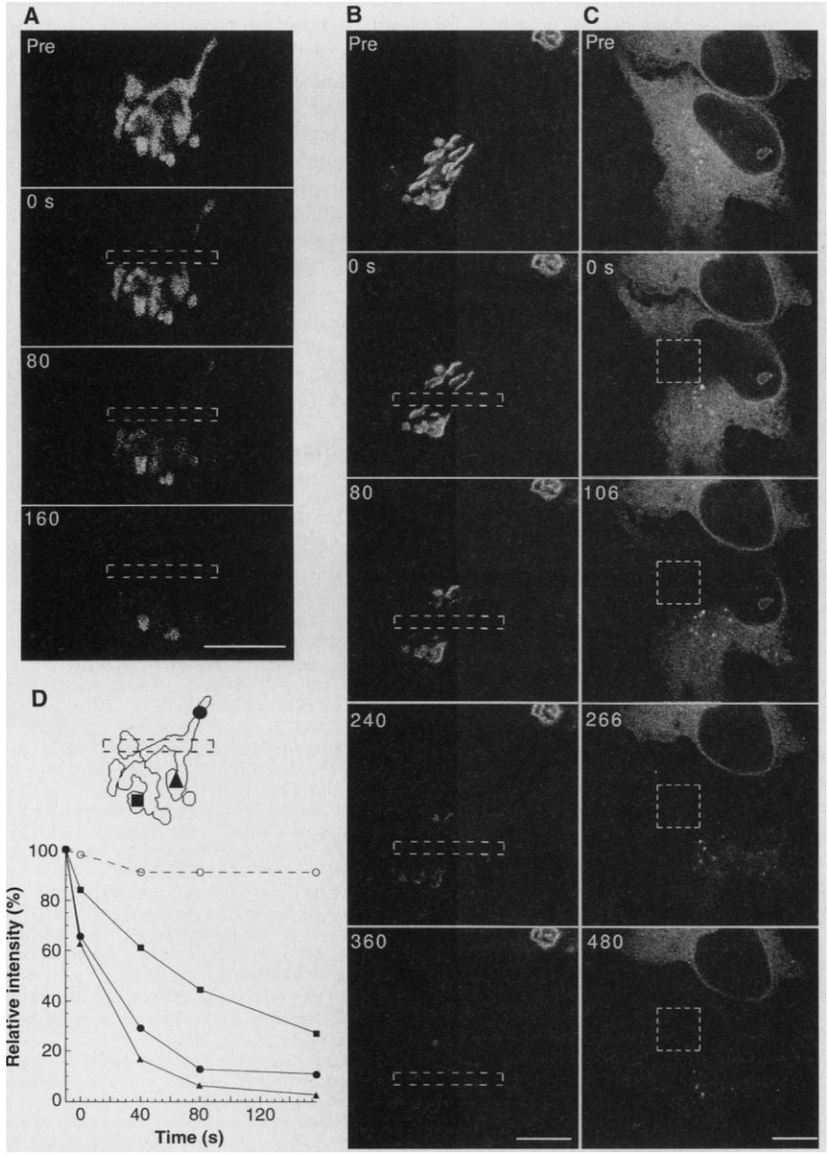

Fig. 3. FLIP of GalTase-GFP in Golgi and ER membranes. HeLa cells expressing GalTase-GFP were untreated (**A** and **B**) or treated with BFA (2 μg/ml) for 30 min (**C**) before the FLIP experiment, which was performed on a 37°C stage of a Zeiss LSM 410 microscope. A small rectangular region defined by the boxed area was repeatedly illuminated with the highest energy of the laser (100% power, 100% transmission, scan time of 30 s). Between each intense illumination, the entire field of view was imaged at low-power laser light (10% power, 3% transmission) to assess the extent that fluorescence outside the box was lost as a consequence of photobleaching within the box. In (A) and (B), areas of Golgi adjacent to the boxed area that was photobleached rapidly lost fluorescence, but a Golgi in an adjacent cell [(B), upper right hand corner] remained bright. Different zones within the Golgi in (A) lost fluorescence at different rates. The rate of fluorescence loss for three selected areas is plotted in (**D**). The open circles (D) show the intensity of fluorescence at the same time points in the Golgi of an adjacent cell, which remained bright. In (C), FLIP of a zone within the ER gradually depleted fluorescence from the entire ER of the affected cell, but not the adjacent cell above it. That Golgi and ER membranes inside the bleached zone were not damaged during exposure to the intense light was confirmed by fixing cells after photobleaching and staining with Golgi-specific antibodies, which revealed intact Golgi and ER structures. The possibility that regions on the edge of the illuminated zone are progressively bleached by light leakage during FLIP was ruled out by repeat of FLIP on fixed cells, which showed bleaching only in the area exposed to intense light illumination. Scale bars = 10 μm. A Quicktime movie sequence from the FLIP experiment is available at http://www.uchc.edu/htterasaki/flip.html.

In contrast to cells in control medium, the Golgi of cells treated with aluminum fluoride (AlF) for 30 min showed essentially no recovery from photobleaching (Fig. 2B). This effect of AlF appeared to be specific to Golgi because GFP chimeras localized within the ER after BFA treatment recovered normally after photobleaching in the presence of AlF (Fig. 2C). AlF is known to cause extensive binding of peripheral protein complexes to Golgi membranes, similar to the effects of guanosine 5′-*O*-(3′-thiotriphosphate) (GTP-γ-S) (*13*), which could constrain the lateral movement of Golgi membrane proteins (*14*).

Quantitative studies of the mobility of the chimeras were carried out with a conventional (nonscanning) light microscope and laser system designed for FPR experiments (Table 1). Fluorescence loss and recovery was measured in a 2-μm stripe placed across the Golgi of individual cells at random orientations. The diffusion coefficients, D, calculated from these measurements ranged from 3×10^{-9} to 5×10^{-9} cm^2 s^{-1}. These values are comparable with the largest D known for any cell membrane protein, that for rhodopsin in rod outer segments (*15*). They are three to five times those reported for antibody-labeled vesicular stomatitis virus G glycoprotein in the Golgi complex (*16*), and they are 10 to 30 times the D measured for many plasma membrane proteins, whose lateral mobility is typically constrained by interactions with each other, with components of the extracellular matrix, or with the cytoskeleton (*15*). The high D values indicate that the lateral diffusion of the GFP chimeras in Golgi membranes was not hindered by interactions such as aggregation with other proteins.

The exceptionally high mobile fraction and diffusion coefficients of the GFP chimeras prompted us to investigate the extent to which Golgi membranes are continuous and whether all regions of the Golgi complex can contribute to recovery of fluorescence at a bleached site. A variation of FPR was used in which fluorescence loss outside the photobleached zone was monitored

(called FLIP for fluorescence loss in photobleaching). A narrow box across the Golgi complex was bleached repeatedly and the fluorescence loss in Golgi membranes outside this box was followed over time. The GalTase-GFP fluorescence associated with Golgi elements extending outside the box was lost completely after 10 intense illuminations of the boxed region (elapsed time was 360 s) (Fig. 3B). This observation suggested that during this time period nearly all of the GalTase-GFP had diffused into the box to become photobleached. The Golgi complex at the upper right-hand corner of Fig. 3B, which was contained within an adjacent cell, remained bright, indicating that the low-intensity laser illumination used for imaging between bleaching radiations led to minimal photobleaching. In some cells, fluorescence associated with particular Golgi sites near the bleached line was lost at different rates (Fig. 3, A and D), suggesting differences in local densities or connectedness (or both) of adjacent Golgi stacks. Movement of GalTase-GFP between Golgi stacks appeared to be mediated by lateral diffusion rather than vesicular transport because FLIP was not slowed at 22°C or by energy depletion (*17*).

The FLIP experiments (*18*) were consistent with the exceptionally high mobility and diffusion rates of the GFP chimeras in Golgi membranes measured in the FPR studies, and the results imply that Golgi stacks normally are extensively interconnected, with Golgi membrane components moving rapidly from one part of the Golgi to another. Previous studies have demonstrated lateral movement of lipid, but not of protein, across the Golgi (*19*). The tubulovesicular elements seen connecting membranes of adjacent Golgi stacks in ultrastructural studies (*20*) could be the conduit by which these proteins and lipids diffuse between adjacent Golgi stacks. FLIP offers a simple method for providing insight into the nature and role of these membrane connections by revealing conditions of and rates of interstack diffusion. Because individual Golgi cisternae are not selectively photobleached in the FLIP experiments, the question remains as to whether intercisternal diffusion occurs within a single stack (*21*).

FLIP experiments were also used to investigate the mobility of GalTase-GFP redistributed into the ER by BFA (Fig. 3C). Repeated photobleaching of a small rectangular region of the ER over 480 s resulted in the complete loss of ER-associated fluorescence from the photobleached cell (including its nuclear envelope). Thus, GalTase-GFP was free to diffuse throughout ER membranes, and all membranes of this compartment are completely interconnected, as expected (*22*).

To test whether the diffusibilities of the GFP chimeras in ER membranes were similar to those in Golgi membranes, we measured *D* by FPR of chimeras redistributed into the ER by either BFA treatment or overexpression of lysozyme-KDEL. Diffusion of the chimeras within ER membranes also was rapid with *D* ranging from 2.1×10^{-9} to 4.5×10^{-9} cm^2 s^{-1} (Table 1), although *D* values for GalTase and KDELR (with overexpressed ligand) were only half as large as in Golgi membranes. Whether the lower *D* for these proteins reflects differences in their physical properties and interactions with luminal ER proteins, or reflects differences in the geometry of ER and Golgi membranes, remains to be determined.

These results have important implications for our understanding of Golgi membrane protein retention and mobility. The GFP-tagged proteins all diffused rapidly and freely within Golgi membranes, as well as within ER membranes. The high *D* and mobile fraction of these proteins appear inconsistent with mechanistic explanations of Golgi protein targeting and retention by means of the formation of large, relatively immobile protein complexes (*2*, *23*). Furthermore, rapid and widespread loss of fluorescence from the Golgi upon repeated bleaching of a small zone within the complex implies significant lateral diffusion rather than vesicular transport of the GFP-tagged proteins between Golgi stacks. Golgi models (*24*) thus need to account for how Golgi membranes maintain their identity amidst rapid diffusion of resident components, and they need to explain the role played by these dynamic membrane properties in Golgi structure and function.

Table 1. Diffusion coefficients (*D*) of GFP chimeras in Golgi and ER membranes. HeLa cells were transfected with GalTase-GFP, Man II–GFP, KDELR-GFP, or KDELR$_m$-GFP cDNAs with or without lysozyme-KDEL (ligand) cDNA to allow expression of the chimeras. Cells were treated with or without BFA (2 μg/ml, for 30 min) before photobleaching (*25*). *D* for Man II–GFP was obtained for cells at 37°C, whereas for GalTase-GFP, KDELR-GFP, and KDELR$_m$-GFP, *D* was obtained for cells at 22°C. *D* measured at 37°C for GalTase-GFP, KDELR-GFP, and KDELR$_m$-GFP closely resembled the values obtained at 22°C. The geometric assumption for calculating *D* was that recovery is due to one-dimensional diffusion (*25*). Percentage recovery of fluorescence was 60 to 70% in Golgi and 80 to 90% in ER. This difference in recovery is likely because photobleaching removed a significant proportion of total fluorescence from the Golgi but not from the ER. The standard error of the mean is indicated for each chimera and condition.

Chimera	Location	Condition	*D* value ($\times 10^{-9}$ cm^2 s^{-1})	Number measured
Man II–GFP	Golgi	Untreated	3.2 ± 0.3	18
GalTase-GFP	Golgi	Untreated	5.4 ± 0.4	22
GalTase-GFP	ER	BFA	2.1 ± 0.2	24
KDELR-GFP	Golgi	Untreated	4.6 ± 0.5	14
KDELR-GFP	ER	BFA	4.3 ± 0.5	15
KDELR-GFP	ER	+ Ligand	2.6 ± 0.3	15
KDELR$_m$-GFP	Golgi	Untreated	4.6 ± 0.5	15
KDELR$_m$-GFP	Golgi	+ Ligand	4.6 ± 0.4	24
KDELR$_m$-GFP	ER	BFA + Ligand	4.5 ± 0.5	38

REFERENCES AND NOTES

1. I. Mellman and K. Simons, *Cell* **68**, 829 (1992); T. Nilsson and G. Warren, *Curr. Opin. Cell Biol.* **6**, 517 (1994); S. Munro, *EMBO J.* **14**, 4695 (1995).
2. T. Nilsson, P. Slusarewicz, M. H. Hoe, G. Warren, *FEBS Lett.* **330**, 1 (1993); C. E. Machamer, *Curr. Opin. Cell Biol.* **5**, 606 (1993).
3. M. S. Bretscher and S. Munro, *Science* **261**, 1280 (1993).
4. M. R. Jackson, T. Nilsson, P. A. Peterson, *J. Cell Biol.* **121**, 317 (1993); J. P. Luzio and G. Banting, *Trends Biochem. Sci.* **18**, 395 (1993).
5. M. Edidin, in *Mobility and Proximity in Biological Membranes*, S. Damjanovich, M. Edidin, J. Szollosi, L. Tron, Eds. (CRC Press, Boca Raton, FL, 1994), pp. 109–135.
6. D. C. Prasher, V. K. Eckenrode, W. W. Ward, F. G. Prendergast, M. J. Cormier, *Gene* **15**, 111 (1992); M. Chalfie, Y. Tu, G. Euskirchen, W. W. Ward, D. C. Prasher, *Science* **263**, 802 (1994).
7. Previous work suggested that Man II forms large oligomers within Golgi cisternae (*2*), which could constrain its mobility. In contrast, KDELR, in the absence of bound ligand, is not thought to oligomerize or be constrained in its membrane mobility (*8, 9*).
8. M. J. Lewis and H. R. B. Pelham, *Cell* **68**, 353 (1992).
9. F. M. Townsley, D. W. Wilson, H. R. B. Pelham, *EMBO J.* **12**, 2821 (1993).
10. The GFP coding region from cDNA pGFP10.1 (*6*), in which Ser^{65} was mutated to Thr [R. Heim, A. B. Cubitt, R. Y. Tsien, *Nature* **373**, 663 (1995)], was placed downstream of coding sequences containing murine Golgi α-mannosidase II [K. W. Moremen and P. W. Robbins, *J. Cell Biol.* **115**, 1521 (1991)], human galactosyltransferase [K. A. Masri, H. E. Appert, M. N. Fukuda, *Biochem. Biophys. Res. Commun.* **157**, 657 (1988)], or wild-type or a mutant form of the human homolog of the yeast ERD2 receptor, ELP1 [V. W. Hsu, N. Shah, R. D. Klausner, *Cell* **69**, 625 (1992)], also known as KDELR. All constructs were generated by standard one- or two-stage polymerase chain reaction methods. Man II–GFP contains full-length Man II, including the NH_2-terminal cytoplasmic tail, uncleaved signal sequence, and complete lumenal domain, followed by the 13–amino acid MYC-derived epitope fused to full-length GFP. GalTase-GFP contains amino acids 1 through 60 of human galactosyltransferase, including the NH_2-terminal cytoplasmic tail, uncleaved signal sequence, and 17 amino acids of the luminal domain fused to full-length GFP. KDELR-GFP contains the full-length coding sequence of ELP1, followed by the 13–amino acid MYC-derived epitope, followed by full-length GFP. KDELR$_m$-GFP was generated by mutagenizing the aspartic acid to an asparagine residue at position 195 of ELP1, which is analogous to the mutation at

position 193 in ERD2 described in (9). All constructs were subcloned into the expression vectors pCDLSRα or pcDNA1 (Invitrogen) and transiently expressed in HeLa cells.
11. J. Lippincott-Schwartz *et al.*, *Cell* **60**, 821 (1990).
12. Energy depletion was performed as described [J. Donaldson *et al.*, *J. Cell. Biol.* **111**, 2295 (1990)]. This treatment dissociates coatomer complexes (which are believed to mediate vesicle traffic) from Golgi membranes of living cells, blocks export of proteins out of the ER, and prevents processing of newly synthesized proteins by Golgi enzymes. For further discussion of the inhibitory effects of energy depletion and reduced temperature on vesicle traffic, see C. J. Beckers *et al.*, *Cell* **50**, 523 (1987) and E. Kuismanen and J. Saraste, *Methods Cell Biol.* **32**, 257 (1989).
13. J. Donaldson *et al.*, *J. Cell Biol.* **112**, 579 (1991); P. Melancon *et al.*, *Cell* **51**, 1053 (1987).
14. AlF also transforms Golgi membranes into an array of coated buds and vesicles after 30 min of treatment, which could disrupt their continuity (P. Peters, L. Yuan, R. Klausner, J. Lippincott-Schwartz, unpublished electron microscope observations).
15. M. L. Wier and M. Edidin, *J. Cell Biol.* **103**, 215 (1986).
16. B. Storrie, R. Pepperkok, E. H. Stelzer, T. E. Kreis, *J. Cell Sci.* **107**, 1309 (1994).
17. An additional argument that vesicular traffic does not play a major role in the observed movement of the GFP chimeras during FLIP is that vesicles traveling through the cytoplasm should have an equal probability of fusing with acceptor membranes in stacks that are equidistant from a donor membrane. We found, however, that some stacks show very little loss of fluorescence during FLIP compared with others, even though they are equidistant from the zone of photobleaching. Moreover, there appears to be little or no interstack communication after microtubule depolymerization, when Golgi stacks reversibly scatter throughout the cytoplasm. These results are difficult to explain by vesicle traffic but are easily explained by differences in lateral continuities between Golgi stacks.
18. FLIP experiments at 37°C with cells expressing Man II–GFP and KDELR-GFP also showed loss of fluorescence throughout the Golgi complex, suggesting that these molecules diffuse rapidly between Golgi stacks. In cells expressing GFP chimeras in the Golgi, FLIP of a region of the cytoplasm that did not contain Golgi, but presumably did contain ER, did not result in significant loss of Golgi fluorescence over this time frame, suggesting that Golgi membranes are not in direct continuity with the ER.
19. M. S. Cooper, A. H. Cornell-Bell, A. Chernjavsky, J. W. Dani, S. J. Smith, *Cell* **61**, 135 (1990).
20. A. Rambourg and Y. Clermont, *Eur. J. Cell Biol.* **51**, 189 (1990); G. Griffiths *et al.*, *J. Cell Biol.* **108**, 277 (1989); P. Weidman, R. Roth, J. Heuser, *Cell* **75**, 123 (1993); K. Tanaka, A. Mitsushima, H. Fukudome, Y. Kashima, *J. Submicrosc. Cytol.* **18**, 1 (1986).
21. J. E. Rothman and G. Warren, *Curr. Biol.* **4**, 220 (1994); P. J. Weidman, *Trends Cell Biol.* **5**, 302 (1995).
22. L. A. Jaffe and M. Terasaki, *Dev. Biol.* **156**, 556 (1993).
23. The data, however, do not rule out the possibility that native Man II and GalTase ever oligomerize. They only indicate that such complex formation is not required for efficient Golgi targeting and retention of these proteins.
24. As one example, for models that assume the existence of functionally discrete Golgi cisternae or subcompartments [J. E. Rothman and L. Orci, *Nature* **355**, 409 (1992)], our findings would imply that mechanisms exist for ensuring that membrane continuities between adjacent stacks only form between homologous membranes (that is, cis to cis and trans to trans). Otherwise, Golgi cisternae within a Golgi stack could not remain completely separate and distinct from each other.
25. The microscope system described in (*15*) was used in the quantitative FPR experiments. The FPR beam was imaged into the sample as a stripe 2 μm wide. Because the stripe extended across the entire width of the Golgi or ER and bleached through the whole depth, diffusion was into and out of a line bounded on its sides, and not on its end. Hence, recovery of fluorescence was due to one-dimensional diffusion. The imposition of one-dimensional geometry on a complicated membrane as well as the mathematics for this case are covered in C.-L. Wey, M. A. Edidin, R. A. Cone, *Biophys. J.* **33**, 225 (1981). Briefly, a tortuous diffusion path reduces the apparent *D*, so our measurements in that case would be an underestimation.
26. Cells were transfected with GFP chimera cDNAs by $CaPO_4$ precipitation. Fluorescent cells were imaged at 37°C in buffered medium with a Zeiss LSM 410 confocal microscope system having a 100× Zeiss planapo objective (NA 1.4). The GFP molecule was excited with the 488 line of a krypton-argon laser and imaged with a 515–540 bandpass filter. Images were transferred to a Macintosh computer for editing and were printed with a Fujix Pictrography 3000 Digital Printer.
27. We thank R. Klausner, E. Siggia, J. Bonifacino, J. Zimmerberg, J. Donaldson, J. Presley, J. Ellenberg, and K. Zaal for valuable comments and suggestions, and M. Chalfie, K. Moremen, M. Fukuda, R. Poljak, and V. Hsu for generous gifts of reagents. M.E. is supported by grant R37 AI14584. Quicktime movies are available at http://www.uchc.edu/hterasaki/flip.html.

22 March 1996; accepted 20 May 1996

Central Hypotensive Effects of the α_{2a}-Adrenergic Receptor Subtype

Leigh B. MacMillan, Lutz Hein, Marta S. Smith, Michael T. Piascik, Lee E. Limbird*

α_2-Adrenergic receptors (α_2ARs) present in the brainstem decrease blood pressure and are targets for clinically effective antihypertensive drugs. The existence of three α_2AR subtypes, the lack of subtype-specific ligands, and the cross-reactivity of α_2AR agonists with imidazoline receptors has precluded an understanding of the role of individual α_2AR subtypes in the hypotensive response. Gene targeting was used to introduce a point mutation into the α_{2a}AR subtype in the mouse genome. The hypotensive response to α_2AR agonists was lost in the mutant mice, demonstrating that the α_{2a}AR subtype plays a principal role in this response.

α_2ARs located in the rostral ventrolateral medulla respond to norepinephrine and epinephrine to decrease sympathetic outflow and reduce arterial blood pressure (*1*). This hypotensive effect has been the rationale for the use of clonidine, an α_2AR agonist, in the treatment of hypertension (*1*). There is controversy, however, concerning whether agents such as clonidine, which contain an imidazole moiety, elicit their hypotensive effects by interacting with α_2ARs or with a separate so-called imidazoline receptor population (*2*). Endogenous agonists of the putative imidazoline receptor population have been described (*3*). We explored the role of α_{2a}AR, one of three α_2AR subtypes (*4*), in eliciting a hypotensive effect because brainstem localization of α_{2a}AR mRNA suggested that the α_{2a}AR subtype might participate in this response (*5*).

We used gene targeting to mutate the α_{2a}AR gene to express an $Asp^{79}\rightarrow Asn$ (D79N) α_{2a}AR in mice. The D79N mutation substitutes asparagine for the aspartate residue at position 79, which is predicted to lie within the second transmembrane span of α_{2a}AR and is highly conserved among heterotrimeric GTP-binding protein (G protein)–coupled receptors (*6*). In AtT20 anterior pituitary cells, the D79N α_{2a}AR is selectively uncoupled from activation of K^+ currents, but remains coupled to inhibition of voltage-gated Ca^{2+} channels and of adenosine 3′,5′-monophosphate (cAMP) production characteristic of the wild-type receptor (*7*). We created a mouse line with this D79N α_{2a}AR to explore both the role of the α_{2a}AR subtype in cardiovascular and other physiological functions and the role of various signal-transduction pathways in α_{2a}AR effects. We now report the cardiovascular functions of this mutant D79N α_{2a}AR.

The substitution of the mutant for the wild-type α_{2a}AR gene in the mouse genome (*8*) was documented by Southern (DNA) analysis of diagnostic restriction digests in offspring of heterozygous intercrosses (Fig. 1A) and by DNA sequencing (Fig. 1B). The density of α_{2a}AR, assessed through use of the ^{3}H-labeled α_2AR antagonist RX 821002, was significantly reduced (80%) in mice homozygous for the D79N α_{2a}AR compared with wild-type mice (Fig. 2A). This reduction in density was not caused by changes in the amount of mRNA encoding D79N α_{2a}AR (Fig. 2B). These findings indicate that, in vivo, the D79N α_{2a}AR is improperly processed or stabilized in target cells. α_{2a}AR binding properties in mutant animals, however, showed appropriate α_{2a}AR selectivity and the absence of allosteric

L. B. MacMillan and L. E. Limbird, Department of Pharmacology, Vanderbilt University, Nashville, TN 37232, USA.
L. Hein, Departments of Medicine, and Molecular and Cellular Physiology, Stanford University, Stanford, CA 94305, USA.
M. S. Smith and M. T. Piascik, Department of Pharmacology, University of Kentucky, Lexington, KY 40536, USA.
*To whom correspondence should be addressed.